

# Towards the development of an efficient low-NO<sub>x</sub> ammonia combustor for a micro gas turbine

Ekenechukwu C. Okafor<sup>a,\*</sup>, K.D. Kunkuma A. Somarathne<sup>a</sup>,  
Akihiro Hayakawa<sup>a</sup>, Taku Kudo<sup>a</sup>, Osamu Kurata<sup>b</sup>, Norihiko Iki<sup>b</sup>,  
Hideaki Kobayashi<sup>a</sup>

<sup>a</sup> *Institute of Fluid Science, Tohoku University, 2-1-1 Katahira, Aoba-ku, Sendai 980-8577, Japan*

<sup>b</sup> *Research Institute for Energy Conservation, National Institute of Advanced Industrial Science and Technology (AIST),  
1-2-1 Namiki, Tsukuba, Ibaraki 305-8564, Japan*

Received 1 December 2017; accepted 19 July 2018

Available online 12 August 2018

---

## Abstract

Recent studies have demonstrated stable generation of power from pure ammonia combustion in a micro gas turbine (MGT) with a high combustion efficiency, thus overcoming some of the challenges that discouraged such applications of ammonia in the past. However, achievement of low NO<sub>x</sub> emission from ammonia combustors remains an important challenge. In this study, combustion techniques and combustor design for efficient combustion and low NO<sub>x</sub> emission from an ammonia MGT swirl combustor are proposed. The effects of fuel injection angle, combustor inlet temperature, equivalence ratio, and ambient pressure on flame stabilization and emissions were investigated in a laboratory high pressure combustion chamber. An FTIR gas analyser was employed in analysing the exhaust gases. Numerical modeling using OpenFOAM was done to better understand the dependence of NO emissions on the equivalence ratio. The result show that inclined fuel injection as opposed to vertical injection along the combustor central axis resulted to improved flame stability, and lower NH<sub>3</sub> and NO<sub>x</sub> emissions. Numerical and experimental results showed that a control of the equivalence ratio upstream of the combustor is critical for low NO<sub>x</sub> emission in a rich-lean ammonia combustor. NO emission had a minimum value at an upstream equivalence ratio of 1.10 in the experiments. Furthermore, NO emission was found to decrease with ambient pressure, especially for premixed combustion. For the rich-lean combustion strategy employed in this study, lower NO<sub>x</sub> emission was recorded in premixed combustion than in non-premixed combustion indicating the importance of mixture uniformity for low NO<sub>x</sub> emission from ammonia combustion. A prototype liner developed to enhance the control and uniformity of the equivalence ratio upstream of the combustor further improved ammonia combustion. With the proposed liner design, NO<sub>x</sub> emission of 42 ppmv and ammonia combustion efficiency of 99.5% were achieved at 0.3 MPa for fuel input power of 31.44 kW.

© 2018 The Combustion Institute. Published by Elsevier Inc. All rights reserved.

**Keywords:** Ammonia; Carbon-free fuel; Gas turbine; Low-NO<sub>x</sub> combustor

---

\* Corresponding author.

E-mail address: [okafor@flame.ifs.tohoku.ac.jp](mailto:okafor@flame.ifs.tohoku.ac.jp) (E.C. Okafor).

## 1. Introduction

Previous studies reported challenges associated with ammonia combustion [1,2]. Ammonia–air mixtures have a low burning velocity that is about five times lower than that of methane–air mixtures at stoichiometric condition and NTP [3]. Pratt [1] reported that the low burning velocity of ammonia–air mixtures required low inlet velocities to ensure a sufficiently long fluid residence time in their gas turbine combustor; hence, it discouraged efficient turbulent mixing. Consequently, stabilization of the flame was inhibited leading to an “unacceptably low” ammonia combustion efficiency. Furthermore, the N atom in ammonia molecule may lead to high fuel NO emission [4]. These combustion challenges had discouraged interest in ammonia as a fuel until recently.

Interest in ammonia as a hydrogen carrier was recently kindled in a search for better means of hydrogen transportation and storage. This was accompanied by a renewed interest in ammonia and ammonia–hydrocarbon mixtures as fuels [5,6]. Ammonia can be produced from renewable sources, burns with no carbon oxide emission and has an already established global production and transportation network. Hence, ammonia can be a sustainable alternative fuel, which offers potentials for mitigating greenhouse gases emission from combustion. Hayakawa et al. [7] and Somarathne et al. [8] showed in their experimental and numerical studies, respectively, that premixed  $\text{NH}_3$ –air flames can be stabilized using swirl combustors. Kurata et al. [4] demonstrated efficient power generation from ammonia-fired 50 kWe-class MGT using a high-swirl non-premixed combustor (swirl number = 0.88) originally designed for kerosene combustion. The fuel was injected vertically along the combustor central axis with a surrounding swirling air flow. A heat recuperator was used to raise the combustor inlet temperature (CIT) above 700 K to improve the combustion and thermal efficiencies. The authors recorded NO emission at 16%  $\text{O}_2$  concentration in the order of 1000 ppmv, which is significantly higher than the Japanese regulatory limit of 70 ppmv [14], and employed a large size selective catalytic NO reduction (SCR) system to reduce the NO from the combustor.

Recent developments thus indicate that ammonia–air flames can be successfully stabilized using strong swirling flows. Swirl primarily creates an internal recirculation zone, which circulates hot products and active radicals from downstream to upstream of the combustor and also allows for good mixing. Consequently, preheating and continuous ignition of the unburned mixture is enhanced, enabling the stabilization of even flames with relatively low burning velocity [9–11]. In addition, the fluid residence time is increased by the recirculating motion, allowing sufficient time for consumption of the fuel. [12].

However, high fuel NO emission from ammonia flames remains an important challenge in ammonia combustion applications. The oxidation of  $\text{NH}_2$  and  $\text{NH}$  by O, H, and OH may lead to a large amount of NO production primarily through a HNO intermediate [8,13]. It is thus necessary to develop low-NOx ammonia combustors to minimize the cost of manufacturing and maintaining large size SCR systems for ammonia-fired gas turbines in practice. Numerical studies [8] have demonstrated the potential of NOx control from ammonia combustors using two-stage combustion where a globally rich flame condition is maintained upstream of the combustor, i.e. the primary combustion zone, and a globally lean flame condition is maintained downstream of the combustor, i.e. the secondary combustion zone.

In this study, a series of laboratory experiments were conducted to understand the characteristics of ammonia–air flames in a swirl combustor and develop an efficient low NOx ammonia combustor for MGTs. In addition, numerical modelling was done to extend the understanding of the experimental results.

## 2. Experimental apparatus and procedures

The combustor used here was similar to the one employed by Kurata et al. [4] as shown in Fig. 1. It had detachable fuel injectors surrounded by a swirler for air with a swirl number of 0.88. Four fuel injectors with different injection angles,  $\theta$ , to the burner central axis were studied. In this study, non-premixed and premixed combustion were investigated. The combustor could be configured to allow air to flow unrestrictedly to the swirler from the surroundings. On the other hand, the swirler could be sealed off from the surrounding air while four air inlet ports are used to connect the swirler to an air supply. The former configuration was meant for imitating the combustion air inlet pattern employed in MGTs, while the latter was used in experiments where the equivalence ratio of the primary combustion zone was controlled independent of the overall equivalence ratio in the combustor as discussed in Section 4.2.

Three different combustor liners with similar dimensions were employed, namely; the original MGT liner, a prototype liner and a model liner. The original liner had holes meant for film cooling and air dilution in the primary and secondary zones. In addition, gaps existed between the liner and the sleeve-fitted base plate owing to the corrugated circumference of the base plate. The secondary dilution holes enabled a rich-lean combustion strategy as air flowed into the combustor through the holes. The prototype liner was developed from the original liner by closing all holes in the primary combustion zone, including the gaps at the sleeve fitting. The model liner was developed with no

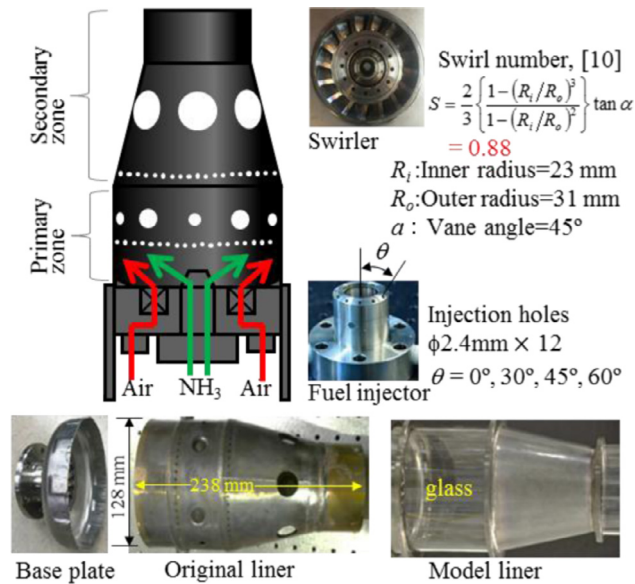


Fig. 1. The MGT high-swirl combustor.

holes and was equipped with quartz glass base and top portions to allow observation of the flame. The model liner was used in experiments where, for simplicity, air dilution was not needed.

The combustor was placed inside a high pressure combustion chamber shown schematically in Fig. 2. The chamber had a design pressure of 1.0 MPa and consisted of three sections with six optical windows on the middle section. Air was supplied through the lower section of the chamber from a 4.5 MPa and 7.5 m<sup>3</sup> air tank with a high-pressure compressor. The air temperature before inlet into the combustor, i.e. the CIT, was controlled using 3 and 12 kW super heaters. To initiate combustion, a glow plug was used to ignite hydrogen gas supplied to the combustor from pressurized cylinders. Gaseous ammonia (> 99.9%) was then supplied from two 50 kg liquid ammonia cylinders while the hydrogen supply was turned off. The flow rates of air and ammonia were measured with Brooks mass flow controllers with accuracies ranging from  $\pm 0.18\%$  to  $\pm 1.00\%$  of full scale (F.S.) depending on the value of F.S. The chamber pressure was manually controlled using valves mounted on the exhaust pipe. The top section of the chamber and the exhaust pipe were water-cooled. Four K-type thermocouples were placed at the liner exit to measure the combustor outlet temperature, (COT).

Emissions were measured using an FTIR (BOB-2000FT) gas analyser with a scanning frequency of 5 Hz and accuracy ranging from  $\pm 1\%$  to  $\pm 2\%$  of F.S., depending on the species. Exhaust gases were sampled from the combustor exit using a 10 mm diameter stainless steel pipe, which was perforated at regular intervals and placed 40 mm above the liner exit. The sampling line was maintain at 464 K to

avoid condensation of water vapour along the line and ensure that chemical reactions were quenched. The sampling flow rate was 2 L/min. For each measurement, data was logged for 2 min and the mean values are reported here. Because the species concentration in the exhaust gases were allowed to attain approximately steady values before data was logged, the standard deviation from the mean at all conditions in this study is not more than 5%.

The possible major sources of uncertainties in the present measurements include uncertainty in measuring the flow rates and emissions. However, uncertainties in flow rate measurements were minimized by choosing mass flow controllers of appropriate F.S. ranges depending on the flow rate measured. Furthermore, the FTIR gas analyser had various measuring ranges for most of the species, which were chosen depending on the magnitude of the emission being measured. Hence, NO, NH<sub>3</sub>, H<sub>2</sub> and O<sub>2</sub> measurements here have uncertainties less than or equal to  $\pm 20\%$  of the measured values. However, uncertainties in N<sub>2</sub>O and NO<sub>2</sub> concentrations are more than  $\pm 20\%$  because the measured values are very low compared to the smallest scale used for their measurement.

For all emission measurements conducted at CIT = 298 K, swirler mean inlet velocity,  $U_{mean}$ , was maintained at 2.70 m/s so that the influence of fluid residence time could be neglected in the comparison of the results. For the measurements at CIT = 500 K,  $U_{mean}$  was maintained at 4.5 m/s.

### 3. Numerical modelling

Large eddy simulation (LES) with a finite rate chemistry was conducted using OpenFOAM [15] in

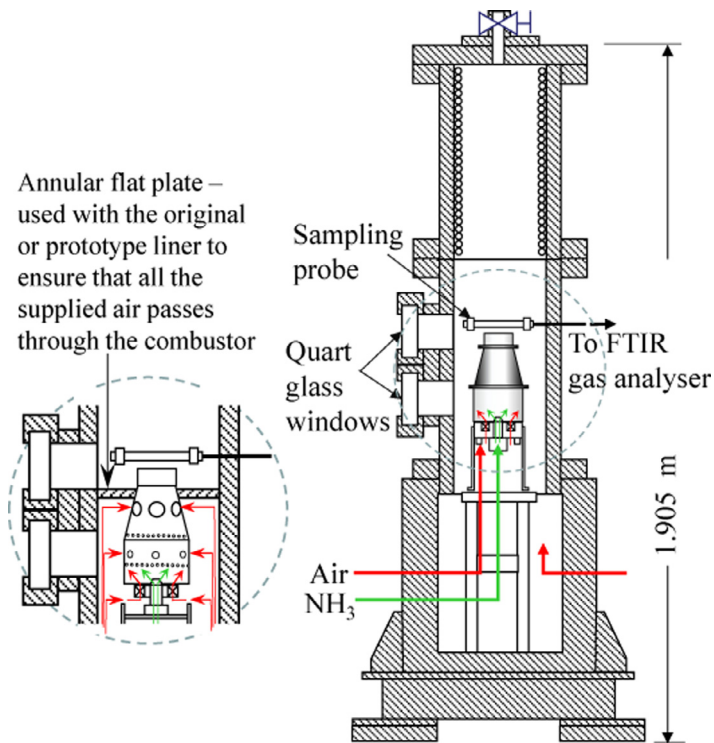


Fig. 2. The high pressure combustion chamber.

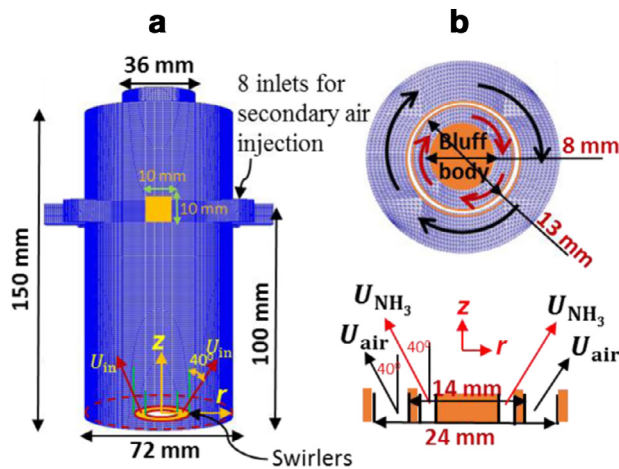


Fig. 3. (a) The computation domain. (b) The dimensions of the swirlers.

order to gain a 3D understanding of the effects of equivalence ratio of the primary zone on emissions from a rich-lean combustor. Somaratne et al. [8] used OpenFOAM in their previous studies to model premixed ammonia–air flames in a gas turbine-like swirl combustor. The numerical methods and the computational domain with a secondary air injection system used in [8] were employed here, with the addition of an inner swirler

for ammonia and outer swirler for air as Fig. 3 shows. Spatially filtered Navier–Stokes equations [16] were solved in the calculations. In LES, scales smaller than the grid size are not resolved but are accounted for through the sub-grid scale tensor, which was modeled based on an eddy-viscosity assumption. The wall adaptive local eddy-viscosity (WALE) model [17] was employed for modeling

the sub-grid scale viscosity. Unresolved fluxes of species and sensible enthalpy in the spatially filtered mass fraction and sensible enthalpy equations were adopted as gradient assumptions. Moreover, a model transport equation for the turbulent kinetic energy [18] was solved for the turbulent combustion modeling. The filtered reaction rate terms were modeled using partially stirred reactor (PaSR) model [19], which accounts for the turbulent-chemistry interaction. The walls of the combustor were non-slip and adiabatic, and the outlet was specified by the continuity boundary condition. An *in-situ* adaptive tabulation algorithm library [20] was combined with the main computational program in order to speed up the calculations.

The reaction mechanism by Tian et al. [21] has been shown to model fuel NO emission from methane–ammonia-fired combustors and also the laminar burning velocity of ammonia–air flames relatively satisfactorily [3,22]. Analysis of the chemistry of one-dimensional ammonia–air flames using ANSYS Chemkin-PRO [23] was done employing the mechanism by Tian et al. [21]. However, the mechanism by Miller et al. [13] was employed in the LES owing to its small size and close agreement with the mechanism by Tian et al. [21] in terms of NO prediction. In the present numerical modeling, CIT was 500 K while the fuel inlet temperature was 300 K. The ambient pressure was 0.5 MPa and total air flow rate was kept constant at 1320 LPM.

It is recognized that the equivalence ratio of the non-premixed flames may vary locally in the combustor. Therefore, the term “global equivalent ratio,  $\Phi$ ” is henceforth used to refer to the average equivalence ratio. In this study,  $\Phi$  is used for both non-premixed and premixed flames. Where stratified combustion (such as rich-lean) strategy was employed,  $\Phi_{\text{overall}}$  refers to  $\Phi$  obtained based on the total air and fuel getting into the combustor while  $\Phi_{\text{primary}}$  refers to  $\Phi$  of the primary combustion zone alone.

## 4. Results and discussion

### 4.1. Ammonia injection angle

The relatively low burning velocity of ammonia–air mixtures may inhibit the stabilization of the flames because ammonia–air mixtures consequently needs a long fuel residence time in the combustor for complete combustion; hence, a low inlet velocity is required. However, low inlet velocity discourages efficient turbulent mixing, which is important for flame stabilization. Pratt [1] proposed that methods that improve mixing in the combustor may improve the combustion efficiency of ammonia. It was found in this study, as discussed below, that the fuel injection angle has a substantial effect on the flame stability because

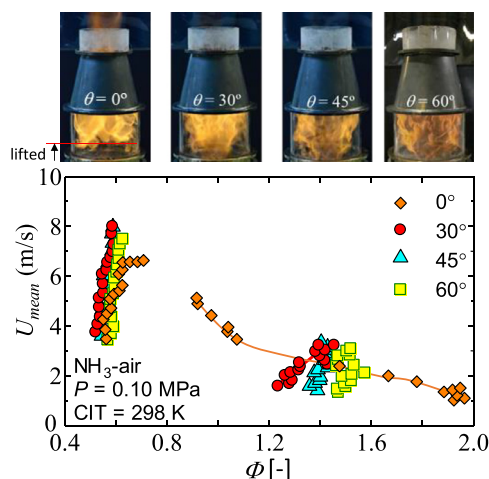


Fig. 4. Blow-off limits of the non-premixed  $\text{NH}_3$ –air flames. The orange flame chemiluminescence is due to the  $\text{NH}_2\alpha$  band and the super-heated  $\text{H}_2\text{O}$  vapour spectra [3]. (For interpretation of the references to color in this figure legend, the reader is referred to the web version of this article.)

it may affect mixing and fuel residence time in the combustor.

Firstly, the blow-off limits of non-premixed ammonia–air flames were measured using the different injectors for CIT of 298 K. The model liner was employed and the blow-off limits were obtained by increasing or decreasing the mean air inlet velocity,  $U_{\text{mean}}$ , at a constant ammonia inlet velocity until a blow-off point was reached. As shown in Fig. 4, images of the flames taken at the same conditions of  $\Phi = 1.0$  and  $U_{\text{mean}} = 2.62$  m/s show that vertical fuel injection resulted in lifted flames with heights more than that of the liner. The region between each pair of curves on the lean and rich side in Fig. 4 is the stability range. The 0° injector had the richest blow-off limits at low  $U_{\text{mean}}$  because a large part of the injected fuel did not mix with air, rather flowed directly to the combustor exit without burning. Therefore, vertical fuel injection discouraged proper mixing, and thus resulted to poor flame stability and large  $\text{NH}_3$  emission. For inclined fuel injection, the rich stability limit was extended as  $\theta$  increased. An increase in  $\theta$  may enhance mixing at the base of the liner because of promoted impingement of the fuel jet on the surrounding strongly swirling air flow. The wide injection angle of the 60° injector promoted combustion closer to the liner walls thereby leading to an undesirable rise in liner temperature above 1300 K. The 45° injector was thus chosen among the inclined injectors for further investigation in this study.

Next, the effect of fuel injection angle on emissions from the combustor was studied, employing a combustion air inlet pattern typical of gas turbine



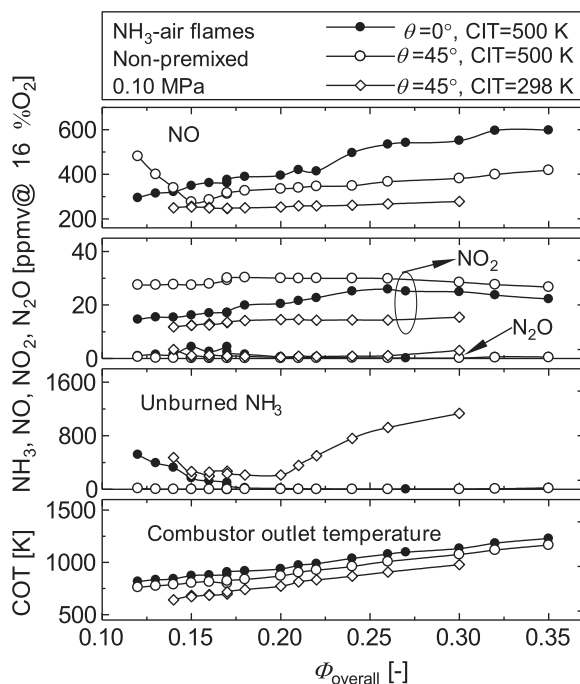


Fig. 5. Variations of emissions and COT with  $\Phi_{\text{overall}}$  for different  $\theta$  and CIT.

combustors. The original MGT liner was used and air was supplied from the base of the high pressure chamber and allowed to flow freely into the various inlets to the combustor including the swirler. An annular flat plate was worn tightly on the slanting shoulder of the liner and tightly fitted to the inner walls of the chamber to ensure that all supplied air from the chamber base passed through the combustor as shown in Fig. 2. The total air flowrate was kept constant at 980 LPM, of which 15.3% passed through the swirler, while the fuel flowrate was varied.

At CIT of 298 K, the  $0^\circ$  injector resulted in unstable flames with ammonia emission more than the largest ammonia measuring range of the FTIR i.e. 5000ppmv. With an increase in CIT to 500 K however, stable ammonia combustion was recorded as Fig. 5 indicates. Ammonia emission was recorded at very low  $\Phi_{\text{overall}}$  due to low flame stability. On the other hand, the  $45^\circ$  injector at CIT of 500 K resulted in more efficient ammonia combustion even at very low  $\Phi_{\text{overall}}$ , and also resulted in lower NO emissions. Furthermore,  $45^\circ$  fuel injection resulted in stable combustion at lower CIT of 298 K; however, unburned ammonia emissions were recorded. The sum of  $\text{NO}_2$  and  $\text{N}_2\text{O}$  concentrations constituted less than 10% of NOx emission from the combustor.

The lower NO emission at CIT of 298 K could be due to the incomplete combustion of ammonia. Note also that unburned ammonia in the flame

may promote NO reduction. On the other hand, analysis of ammonia flame chemistry suggests that lower CIT may result to lower NO production due to; (a) relatively lower rate of NO production from the major fuel NO producing reactions, and (b) relatively higher rate of NO reduction by  $\text{NH}_2$  through  $\text{NH}_2 + \text{NO} = \text{NNH} + \text{OH}$  and  $\text{NH}_2 + \text{NO} = \text{N}_2 + \text{H}_2\text{O}$ . Hence, the more efficient combustion achieved with inclined fuel injection presents potentials for low CIT ammonia combustors, which may produce low levels of NOx.

#### 4.2. Global equivalence ratio

It was confirmed that a control of  $\Phi_{\text{primary}}$  and mixture uniformity are necessary for low NOx emission from ammonia combustors as discussed below. Firstly, the dependence of the emissions on  $\Phi$  was investigated using the model liner and the  $45^\circ$  injector, for both non-premixed and premixed combustion. To ensure comparable fluid residence times at the same  $\Phi$  for both non-premixed and premixed combustion cases, approximately equal flow rates were allowed through the injectors and swirlers in both cases. In the non-premixed case, the air flow rate was kept constant while the fuel flow rate was varied. In the premixed case, fuel and air of quantities equivalent to those used in the corresponding non-premixed condition were premixed and the flow was divided between the swirler and injector in a proportion equivalent to

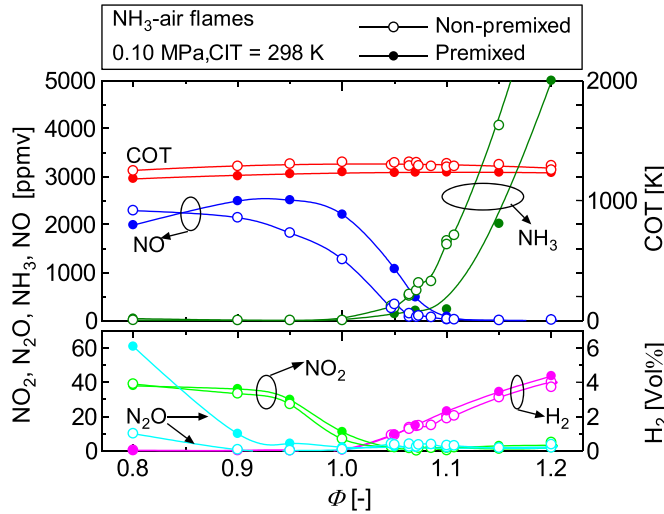


Fig. 6. Variation of measured emissions with global equivalence ratio, without the influence of air dilution.

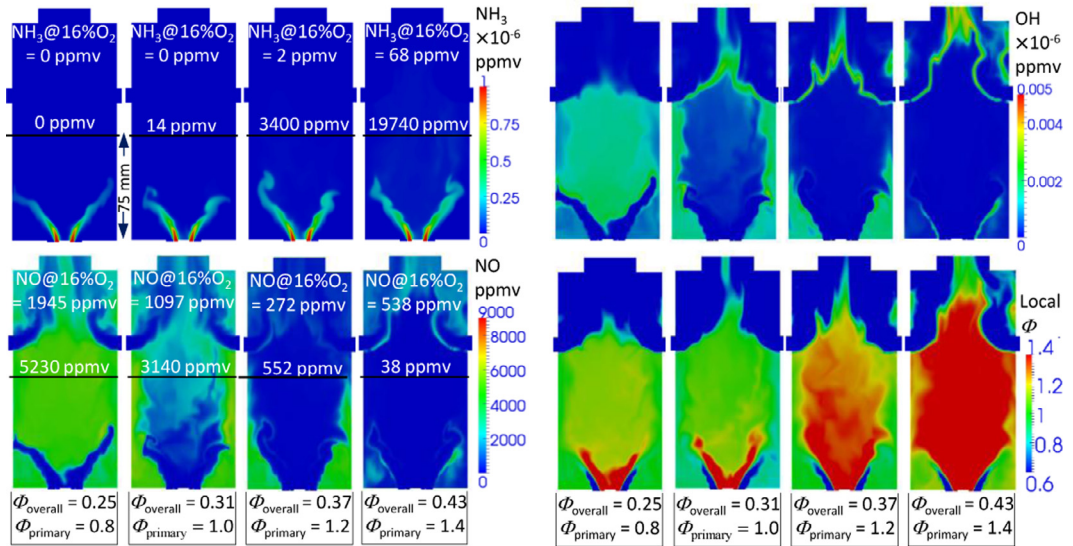


Fig. 7. Profiles of  $\text{NH}_3$ ,  $\text{NO}$ ,  $\text{OH}$  and local equivalence ratio. The space-time average concentrations are indicated at  $Z = 75$  mm and at the combustor exit.

the swirler/injector flow ratio in the corresponding non-premixed case.

Figure 6 shows that lean ammonia–air flames emit high levels of  $\text{NO}$ . Oxidation of  $\text{NH}_i$  by  $\text{O}$ ,  $\text{H}$  and  $\text{OH}$  radicals leads to fuel  $\text{NO}$  production through the  $\text{HNO}$  intermediate [8,13]. Hence, fuel  $\text{NO}$  production is sensitive to the concentration of the  $\text{O}/\text{H}$  radicals. The lower  $\text{NO}$  emission from the rich flames may be due to lower concentrations of these  $\text{O}/\text{H}$  radicals in rich ammonia flames. As the CFD simulation shows in Fig. 7, the  $\text{OH}$  radical profile in the combustor correlates with the  $\text{NO}$  profile and local  $\Phi$  profile. Observe however that

for  $\Phi_{\text{primary}} = 0.8$ ,  $\text{NO}$  concentration is high downstream of the combustor while  $\text{OH}$  concentration is significantly low there because no fuel is burned downstream of the combustor. The high  $\text{NO}$  concentration is from the lean primary zone upstream.

On the other hand, the lower  $\text{NO}$  emission from rich ammonia flames may be due to the promotion of a pathway for  $\text{NH}_2 \rightarrow \text{N}_2$  conversion that does not involve  $\text{NO}$  production, i.e.  $\text{NH}_2 \xrightarrow{+\text{NH}} \text{N}_2\text{H}_2 \xrightarrow{+\text{M,H}} \text{NNH} \rightarrow \text{N}_2$ . The importance of these  $\text{NH}_i$  ( $i = 1, 2$ ) combination reactions in rich ammonia flames and their contribution to lower  $\text{NO}$

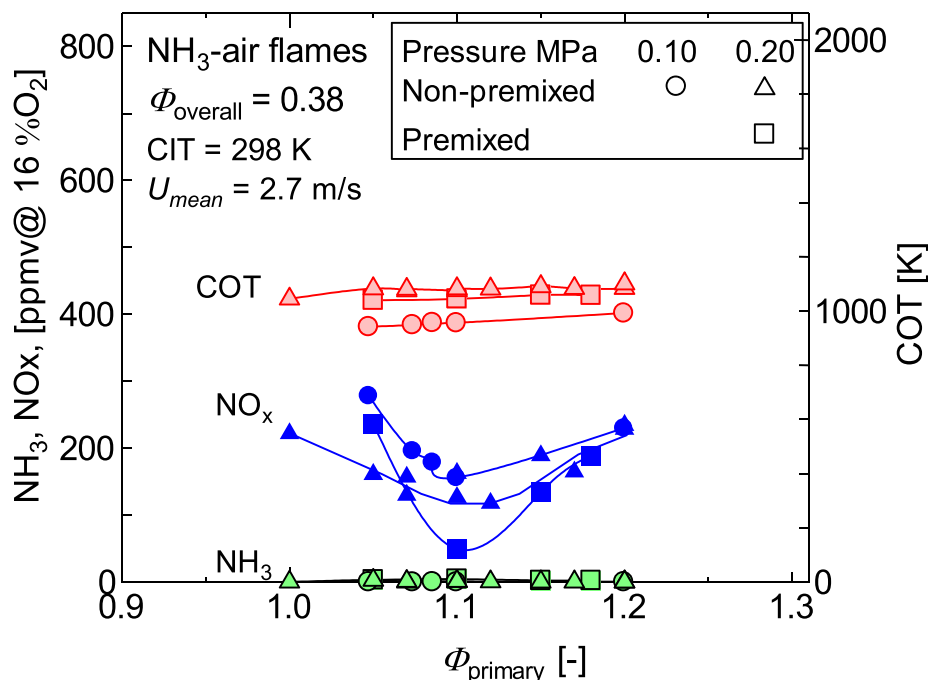


Fig. 8. Variation of  $\text{NO}_x$  and  $\text{NH}_3$  emissions with  $\phi_{\text{primary}}$  at a constant  $\phi_{\text{overall}}$  at different ambient pressures.

production were reported by Dean et al. [24]. Shock tube measurements identified them as the major steps in high temperature decomposition of ammonia in the absence of  $\text{O}_2$  [25]. With the smaller O/H radical pool in rich flames, consumption of  $\text{NH}_i$  via the radical combination route is promoted.

The numerical results in Fig. 7 indicates, as suggested by Fig. 6, that a slightly rich  $\phi_{\text{primary}}$  may ensure low  $\text{NO}$  and  $\text{NH}_3$  emissions from the two-stage rich-lean combustor. When  $\phi_{\text{primary}}$  is lean ( $\phi_{\text{primary}} = 0.8$ ),  $\text{NO}$  emissions is high due to high  $\text{NO}$  production in the primary zone. On the other hand, when  $\phi_{\text{primary}}$  is substantially rich ( $\phi_{\text{primary}} = 1.4$ ),  $\text{NO}$  production in the primary zone is very low; however, significant amounts of unburned  $\text{NH}_3$  is transported to the secondary zone. This large amount of  $\text{NH}_3$  is burned as air is injected in the secondary zone, leading to high  $\text{NO}$  production and emission. Furthermore, as Fig. 6 shows, high levels of  $\text{H}_2$  emission is recorded at rich flame conditions. In the two-stage combustor, the  $\text{H}_2$  is burned in the secondary zone, promoting OH and consequently  $\text{NO}$  production. Unless the  $\text{NH}_3$  and  $\text{H}_2$  are not completely burned in the secondary zone, beyond the slightly rich  $\phi_{\text{primary}}$  with the lowest  $\text{NO}$  emission, overall  $\text{NO}$  emission from the combustor may increase with  $\phi_{\text{primary}}$  because increasing amount of  $\text{NH}_3$  and  $\text{H}_2$  are transported to and burned in the secondary zone.

Therefore, achieving low  $\text{NO}$  emission from the two-stage combustor involves the suppression of

$\text{NO}$  production in the primary and secondary zones through slightly rich combustion in the primary zone. The presence of inlets for air in the primary zone of the original MGT liner may however result to sufficiently large regions of lean combustion in the primary zone with high  $\text{NO}$  production. To ensure a better control and uniformity of  $\phi_{\text{primary}}$  in the combustor therefore, the prototype liner was designed and then employed to investigate the effects of  $\phi_{\text{primary}}$  and  $\phi_{\text{overall}}$  on emissions from the combustor. Note that for the combustion air inlet strategy employed in MGTs,  $\phi_{\text{primary}}$  is proportional to  $\phi_{\text{overall}}$ . Therefore, to study the effects of either equivalence ratios independently, the combustion air inlet strategy was changed. The air passing through the swirler and that through the other holes on the liner were independently controlled.

Figure 8 confirms that a slightly rich  $\phi_{\text{primary}}$  is necessary for low  $\text{NO}_x$  emission from the combustor at different ambient pressures. The optimum low- $\text{NO}_x$   $\phi_{\text{primary}}$  was found to be 1.10. For a constant  $\phi_{\text{primary}}$  of 1.10,  $\text{NO}_x$  emission at 16%  $\text{O}_2$  concentration was found to be insensitive to  $\phi_{\text{overall}}$  over the range of  $\phi_{\text{overall}} = 0.40$  to 0.67 as shown in Fig. 9. The maximum fuel input power in this study was 31.44 kW at 0.30 MPa where the lowest  $\text{NO}_x$  emission of 42  $\text{ppmv}$  with 99.5% combustion efficiency was recorded, as shown in Fig. 9.

By comparing the data in Fig. 5 for  $\text{CIT} = 298 \text{ K}$  with Figs. 8 and 9, it can be concluded that the prototype liner resulted in more efficient



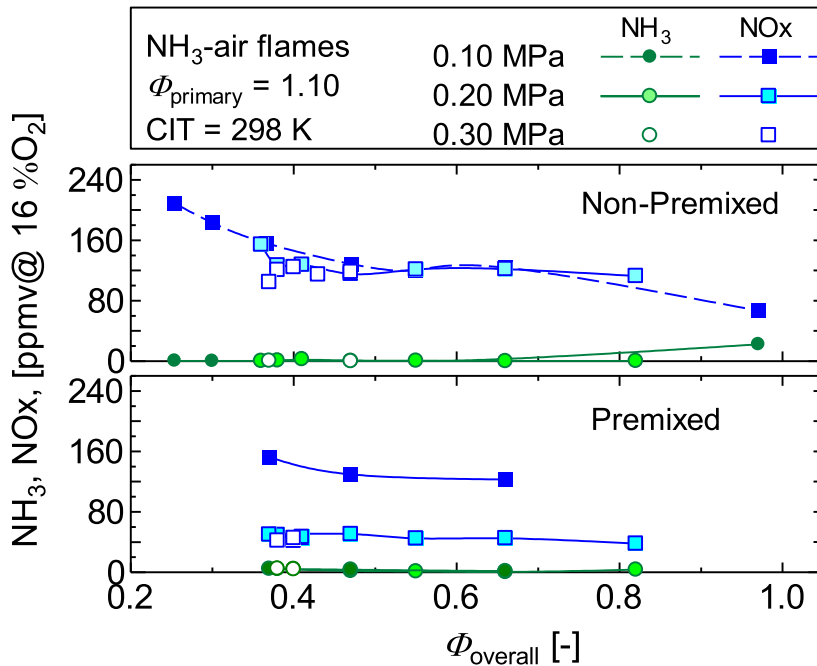


Fig. 9. Variation of NOx and NH<sub>3</sub> emissions with  $\Phi_{\text{overall}}$  at a constant  $\Phi_{\text{primary}}$  at different ambient pressures.

ammonia combustion. This was mainly due to the closing of the sleeve fitting gaps. Air entering the combustor through the gaps flowed along the liner wall without passing through the swirler, thus the flow may exit the combustor without been swirled or recirculated. In other words, streamlines with relatively short residence time in the combustor, which may transport unburned ammonia from the liner base out of the combustor, was created by the gaps.

NO emission from the combustor decreased with an increase in ambient pressure as shown in Fig. 9. An increase in pressure may lead to a depletion of the O/H radicals pool, due mainly to the enhancement of the pressure-sensitive reactions  $\text{H} + \text{OH} + (\text{M}) = \text{H}_2\text{O} + (\text{M})$  and  $\text{H} + \text{O}_2 + (\text{M}) = \text{HO}_2 + (\text{M})$ . Therefore, NH<sub>i</sub> oxidation by the O/H radicals pool may decrease with pressure, and consequently result to a decrease in NO production. Note that NO concentration in ammonia flames has a high negative sensitivity to the rate of  $\text{H} + \text{OH} + (\text{M}) = \text{H}_2\text{O} + (\text{M})$ , and the sensitivity increases with pressure [8]. In addition, NH<sub>i</sub> consumption through the pressure-sensitive NH<sub>i</sub> combination reactions may be promoted thereby promoting the no-NOx pathway discussed previously. On the other hand, a slight decrease in flame height indicating faster fuel consumption was observed with an increase in pressure. This may reduce the amount of unburned NH<sub>3</sub> and H<sub>2</sub> entering the secondary zone to produce NO. The effects of pressure on NO emission from the

combustor may however be due mainly to the effects on flame chemistry.

The lower NOx emission from the premixed combustion in comparison to that from the non-premixed combustion confirms the importance of mixture uniformity for low fuel NOx emission. It should be noted that the primary target of two-stage rich-lean combustion and mixture homogenization in ammonia combustors is to control the distribution of the O/H radicals pool, rather than temperature, which is the case in thermal NOx control. Although temperature may enhance the production of the radicals, other factors such as the profiles of NH<sub>i=0,1,2,3</sub> and H<sub>2</sub> in the combustor, which are primarily controlled by the local equivalence ratio may have dominant effects on the radical distribution and fuel NO production.

## 5. Conclusions

Laboratory studies on the effects of several parameters on the characteristics of an ammonia MGT combustor has been conducted and combustion techniques and design for an efficient low-NOx ammonia combustor are proposed as summarized below.

1. Improvement of mixing and fluid residence time in the combustor by the use of a swirler and inclined fuel injection resulted in improved combustion efficiency even at low CIT, and also resulted in lower emissions.

2. Two-stage rich-lean combustion may result in low NO<sub>x</sub> emission with a high ammonia combustion efficiency when the upstream equivalence ratio is uniform and slightly rich. NO profile in the 3D simulation correlates with the OH and local equivalence ratio profiles indicating that an equivalence ratio control, which may in turn control the O/H radical profiles in the combustor is critical to the control of fuel NO<sub>x</sub> emission.
3. NO<sub>x</sub> emission decreased with ambient pressure especially for the premixed combustion, which had better mixture uniformity. Decrease in O/H radicals concentration with pressure may lead to a decrease in fuel NO<sub>x</sub> production and a promotion of the no-NO<sub>x</sub> NH<sub>2</sub>→N<sub>2</sub> conversion pathway.
4. This study recorded a significantly low NO<sub>x</sub> emission of 42 ppmv with ammonia combustion efficiency of 99.5 % at a CIT of 298 K and fuel input power of 31.44 kW owing to the modifications made to the combustor and the combustion strategies employed.

## Acknowledgment

This research was supported by the Council for Science, Technology and Innovation (CSTI), the Cross-ministerial Strategic Innovation Promotion Program(SIP), “Energy Carriers” (Funding Agency: The Japan Science and Technology Agency (JST)).

## References

- [1] D.T. Pratt, Performance of ammonia-fired gas-turbine combustors, Technical Report No.9, DA-04-200-AMC-791(x), Berkley University of California, 1967, Available at <<http://www.dtic.mil/dtic/tr/fulltext/u2/657585.pdf>>.
- [2] F.J. Verkamp, M.C. Hardin, J.R. Williams, *Proc. Combust. Inst.* 11 (1967) 985–992.
- [3] O. Kurata, N. Iki, T. Matsunuma, T. Inoue, T. Tsujimura, H. Furutani, H. Kobayashi, A. Hayakawa, *Proc. Combust. Inst.* 36 (2017) 3351–3359.
- [4] A. Hayakawa, T. Goto, R. Mimoto, Y. Arakawa, T. Kudo, H. Kobayashi, *Fuel* 159 (2015) 98–106.
- [5] E.C. Okafor, Y. Naito, S. Colson, et al., *Combust. Flame* 187 (2018) 185–198.
- [6] A. Valera-Medina, R. Marsh, J. Runyon, et al., *Appl. Energy* 185 (2017) 1362–1371.
- [7] A. Hayakawa, Y. Arakawa, R. Mimoto, et al., *Int. J. Hydrogen Energy* 42 (2017) 14010–14018.
- [8] K.D.K.A. Somarathne, S. Hatakeyama, A. Hayakawa, H. Kobayashi, *Int. J. Hydrogen Energy* 42 (2017) 27388–27399.
- [9] T. Terasaki, S. Hayashi, *Proc. Combust. Inst.* 26 (1996) 2733–2739.
- [10] N. Syred, *Prog. Energy Combust. Syst* 32 (2) (2006) 93–161.
- [11] A. Valera-Medina, N. Syred, A. Griffiths, *Combust. Flame* 156 (2009) 1723–1734.
- [12] V.M. Reddy, A. Katoch, W.L. Roberts, S. Kumar, *Proc. Combust. Inst.* 35 (2015) 3581–3589.
- [13] J.A. Miller, M.D. Smooke, R.M. Green, R.J. Kee, *Combust. Sci. Tech* 34 (1983) 149–176.
- [14] Ministry of Environment, Government of Japan, Regulatory measures against air pollutants emitted from factories and business sites and the outline of regulations- Emission Standards for soot, dust, and NO<sub>x</sub> (1998) Available at: [https://www.env.go.jp/en/air/aq/air/air4\\_table.html](https://www.env.go.jp/en/air/aq/air/air4_table.html).
- [15] OpenFOAM 1.7.1 (2010) Available at: <http://openfoam.org/version/1-7-1/>.
- [16] T. Poinso, D. Veynante, Theoretical and Numerical Combustion, second ed., R. T. Edwards, Inc., Pennsylvania, USA, 2005, pp. 164–169.
- [17] F. Nicoud, F. Ducros, *Flow Turbul. Combust.* 62 (1999) 183–200.
- [18] S. Menon, P.-K. Yeung, W.-W. Kim, *Comput. Fluids* 25 (1996) 165–180.
- [19] S.M. Correa, *Combust. Flame* 93 (1993) 41–60.
- [20] T. Lucchini, F. Contino, G.D. Errico, *Proc. Combust. Inst.* 33 (2011) 3057–3064.
- [21] Z. Tian, Y. Li, L. Zhang, P. Glarborg, F. Qi, *Combust. Flame* 156 (2009) 1413–1426.
- [22] H. Xiao, A. Valera-Medina, R. Marsh, P.J. Bowen, *Fuel* 196 (2017) 344–351.
- [23] CHEMKIN-PRO 17.2, ANSYS, Inc.: San Diego, 2016.
- [24] A.M. Dean, M. -S Chou, D. Stern, *Int. J. Chem. Kinet.* 16 (1984) 633–653.
- [25] F. Davidson, K. Kohse-Hoinghaus, A.Y. Chang, R.K. Hanson, *Int. J. Chem. Kinet.* 22 (1990) 513–535.